

2D axisymmetric modeling of the HTS insert Nougat in a background magnetic field generated by resistive magnet

J eremie Muzet, Christophe Trophime, Xavier Chaud, Christophe PrudHomme and Vincent Chabannes

Abstract—To accompany the development of High Temperature Superconductor (HTS) magnets at the Laboratoire National des Champs Magn etiques Intenses, we have initiated an activity on implementing numerical models to simulate HTS with the *Feel++* finite element (FE) library used for the simulation of the lab high field resistive magnets. In this work, we give an overview of the status of the implementations. We focus on the modeling of the Nougat HTS – that reached 32.5 Tesla in a resistive magnet background field of 18 Tesla. We present some simulations run in parallel that we carried out: for the current density redistribution in the HTS based on the *T-A* formulation and for the estimation of the critical current as a function of the external applied magnetic field using an iterative algorithm based on *A* formulation. The results were validated using comparison with experiments and numerical estimations from [1].

Index Terms—High temperature superconductors, finite element method, *T-A* formulation, critical current

I. INTRODUCTION

THE Laboratoire National des Champs Magn etiques Intenses (LNCMI) is the French user magnet facility, located on 2 sites: Grenoble and Toulouse. The facility is a member of the European Magnetic Field Laboratory (EMFL). LNCMI Grenoble is embarked in the development of HTS magnet since 2012. We achieved to reach 32.5 T with a Metal-as-Insulation (MI) HTS insert made of a stack of 9 double pancakes [1]. This MI HTS insert, Nougat, was operated up to 14.5 T in a resistive background field of 18 T generated by six Helices and two Bitter magnets developed at LNCMI [2].

In the frame of the European project EMFL, we started a new simulation activity on superconductor magnets to accompany these developments. In this prospect, we have implemented the most commonly used formulations for HTS modelling using some specific tools of the multi-physics toolbox *CFPDES* of the *Feel++* Open-Source library [3] developed in collaboration with IRMA University of Strasbourg.

Submitted for review September 26, 2023.

This work was carried out thanks to funding from the European Union’s Horizon 2020 research and innovation program under Grant Agreement No.951714. Any dissemination of results reflects only the author’s view and the European Commission is not responsible for any use that may be made of the information it contains. (*Corresponding author: J eremie Muzet.*)

J. Muzet, C. Trophime and X. Chaud are with the Laboratoire National des Champs Magn etiques Intenses CNRS, Univ. de Grenoble, UPS, Insa, in Grenoble, France (e-mail: jeremie.muzet@lncmi.cnrs.fr; christophe.trophime@lncmi.cnrs.fr; xavier.chaud@lncmi.cnrs.fr).

C. PrudHomme and V. Chabannes, are with the Cemosis, IRMA, Univ. de Strasbourg, CNRS, in Strasbourg, France (e-mail: christophe.prudhomme@emosis.fr; vincent.chabannes@emosis.fr).

Validations of these models have been performed on examples from the HTS modeling platform [4]. A GitHub repository named *feelpp-hts* containing modeling files reproducing simple cases with *Feel++* is available at [5] as well as the documentation. This includes:

- HTS bulk cylinder model with an external field in 2D and axisymmetric coordinates described in [6];
- HTS wire model with transport current in 2D based on [7], [8];
- Roebel cables model in 2D to estimate the critical current described in [9];
- HTS tapes models in 2D from [10] and in axisymmetric coordinates from [11] using the Homogeneous method.

In future work, we will couple these models with the *HEAT* and *SOLID Feel++* toolbox to account for the temperature and stress dependence of the HTS critical current density J_c .

Note that we choose *Feel++* for HTS modeling as it is already used for the modeling of our resistive magnets. Even if *Feel++* is not as ergonomic as commercial software for setting up simulations, it enables us to have control over the solver strategy (solving method, preconditionner, time and mesh adaptivity). We can also benefit from the seamless parallelism implementation to run the same code on a laptop as well as on High Performance Computing (HPC) facilities. *Feel++* has been used on HPC computer with tens of thousands of cores.

II. MODELS & FORMULATIONS

To model HTS material, the FE method models rely on different formulations of Maxwell’s equations. The more widely used formulations are: the *A-V* formulation based on the magnetic potential vector \mathbf{A} , the *H* formulation based on the magnetic field \mathbf{H} [12]. They have been applied to simulate HTS bulks, wires, or tapes [6], [7], [8], [13]. In more recent publications [14], [10], the *T-A* formulation was proposed to simulate thin layers superconductors as well as methods to simplify the description of the systems allowing to study large-scale systems [11].

A. *T-A* Formulation

The *T-A* formulation is a FE formulation which solves two state variables, the magnetic vector potential \mathbf{A} on the entire

geometry, and the current vector potential \mathbf{T} only on the HTS parts [11]:

$$\nabla \times \frac{1}{\mu} \nabla \times \mathbf{A} = \mathbf{J} \quad (1)$$

$$\nabla \times \rho \nabla \times \mathbf{T} = -\frac{\partial \mathbf{B}}{\partial t} \quad (2)$$

with the current density (A/m^2) $\mathbf{J} = \nabla \times \mathbf{T}$, the magnetic flux density (T) $\mathbf{B} = \nabla \times \mathbf{A}$ and ρ the resistivity (Ωm). ρ is given by the so-called *E-J* power law (see subsection C).

In this formulation, the HTS layers are modelled as 1D elements due to their thinness. The transport current can be enforced in the HTS layers with the following boundary condition for \mathbf{T} on the edges of the tapes:

$$\mathbf{I} = \iint_S \mathbf{J} dS = \iint_S \nabla \times \mathbf{T} dS = \oint_{\partial S} \mathbf{T} dl \quad (3)$$

$$\mathbf{I} = (\mathbf{T}_1 - \mathbf{T}_2)\delta \quad (4)$$

with δ the thickness of the HTS layer and \mathbf{T}_1 and \mathbf{T}_2 the current potential at the extremities of the tapes. This expression is both valid in 2D and axisymmetrical geometries.

B. Homogeneous method

The *T-A* formulation can be homogenized, which means that the HTS pancakes are modeled as an anisotropic material. The simplification of the geometry needs additional considerations: the current density in the pancakes becomes a scaled current density $J_s = \frac{\delta}{\Lambda} \mathbf{J}$, where δ and Λ are respectively the thickness of the HTS layer and the thickness of the entire HTS tape. \mathbf{T} is only defined within the anisotropic material and is forced to have only one component as shown in [11]. We apply a similar boundary condition to (4) to each pancake instead of applying the boundary condition to each tape.

C. E-J power law & critical current density

The electrical resistivity of the HTS material is defined by a highly non-linear formula called the *E-J* power law [15]

$$\mathbf{E} = \rho_{\text{HTS}} \mathbf{J} = \frac{E_c}{J_c(\mathbf{B}, \theta)} \left| \frac{\mathbf{J}}{J_c(\mathbf{B}, \theta)} \right|^{n-1} \mathbf{J} \quad (5)$$

with \mathbf{E} , E_c , $J_c(\mathbf{B}, \theta)$ and n respectively the electrical field (V/m), the critical electrical field (V/m), the critical current density (A/m^2) and a material dependent index.

This relation can be inverted to find the current I_i within each tape Ω_i :

$$\mathbf{J}_i = J_c(\mathbf{B}, \theta) P_i \quad (6)$$

$$\mathbf{I}_i = P_i \int_{\Omega_i} J_c(\mathbf{B}, \theta) d\Omega_i \quad (7)$$

with $P_i = \mathbf{E}_i / E_c * |\mathbf{E}_i / E_c|^{1/n-1}$ and \mathbf{E}_i the electric field, uniform across the cross-section of the i^{th} tape (see [9]).

$J_c(\mathbf{B}, \theta)$ describes an anisotropic dependence of J_c on the magnitude and orientation of \mathbf{B} for the considered HTS material. It depends on the tape design. It is defined by a fit function obtained from measurements. Several of those fits are described in [16], [17], [18] and [19] and can be applied to the models implemented here.

```

2  "models": [{
3    "name": "magnetic_Super",
4    "materials": "Super",
5    "setup": {
6      "coefficients": {
7        "c": "x/mu:x:mu",
8        "a": "1/mu/x:x:mu",
9        "f": "x*materials_J:x:materials_J"
10     }
11   }
12  }]

```

Fig. 1. Implementation of (9) from the *T-A* formulation in *CFPDES* with μ the magnetic permeability and materials_J the current density defined for each material. materials_J is given by $\partial \mathbf{T}_r / \partial z$. The expressions for coefficients a , c and f are multiplied by the jacobian r (here x) to account for axisymmetric coordinates.

```

2  "BoundaryConditions": {
3    "current": {
4      "Dirichlet": {
5        "T1": { "expr": "I/delta:I:delta" },
6        "T2": { "expr": "0" }
7      }
8    }
9  }

```

Fig. 2. Implementation of the boundary conditions described by (4) with δ , the thickness of the HTS layer

III. IMPLEMENTATION

A. *Feel++*

In collaboration with Irma University of Strasbourg, we develop tools in an Open-Source C++ library *Feel++* (Finite Element Embedded Language and Library in C++). This FE library allows to solve partial differential equations (PDEs) using Galerkin methods [20].

Additionally, *Feel++* provides toolboxes used for multi-physics modeling and simulation. With only a CFG and a JSON file, it is possible to configure and run models by defining the relevant physical quantities—such as material properties, loads, constraints, sources, and fluxes. It can be used with *pyFeel++*, a python interface to the *Feel++* library API, that gives us modularity and control over the configuration of the magnets and its various variables.

The toolbox used for HTS modeling is Coefficient Form PDEs (*CFPDES*), similar to the interface with the same name in Comsol. It implements a generic convection-diffusion like equation for 2D geometries:

$$d \frac{\partial u}{\partial t} + \nabla \cdot (-c \nabla u + \alpha u + \gamma) + \beta \cdot \nabla u + a u = f \text{ in } \Omega \quad (8)$$

The coefficients of this generic PDE are set so that they correspond to the actual PDE we want to solve (e.g. Fig. 1). In the next section, we show how to cast *T-A* formulation into this formalism for axisymmetrical geometries.

B. Implementation of axisymmetric formulations

The Nougat HTS insert is modeled as an axisymmetric geometry. In cylindrical coordinates (r, z) , (1) and (2) can be

```

1 {
2   "Jc0": 1.85e11,
3   "b0": 0.93,
4   "k": 0.031,
5   "alpha": 0.62,
6   "B_para": "mag_grad_A_0+mag_A/x:mag_grad_A_0:mag_A:x",
7   "B_perp": "-mag_grad_A_1:mag_grad_A_1",
8   "JcB": "Jc0/(1+sqrt(B_para^2*k^2+B_perp^2))^alpha
9         :Jc0:B_para:B_perp:x:k:alpha"
}

```

Fig. 3. Example of JSON file containing a fit function of the critical current density $J_c(\mathbf{B})$ using the Kim's law described in [16].

rewritten as :

$$\nabla \cdot \left(-\frac{1}{\mu} \nabla \mathbf{A}_\theta \right) + \frac{1}{r^2} \frac{\mathbf{A}_\theta}{\mu} = \frac{\partial \mathbf{T}_r}{\partial z} \quad (9)$$

$$\nabla \cdot \left(-\begin{pmatrix} 0 & 0 \\ 0 & \rho \end{pmatrix} \nabla \mathbf{T}_r \right) = \frac{\partial (\partial_z \mathbf{A}_\theta)}{\partial t} \quad (10)$$

To model (9) with (8), we need to identify the coefficients of (8) to match (9). For that purpose, we use (9) weak formulation:

$$\int_{\Omega} \frac{1}{\mu} \nabla \mathbf{A}_\theta \cdot \nabla \phi r dr dz + \int_{\Omega} \frac{1}{r^2} \frac{\mathbf{A}_\theta}{\mu} \phi r dr dz = \int_{\Omega} \frac{\partial \mathbf{T}_r}{\partial z} \phi r dr dz$$

with ϕ a test function from $H_1(\Omega)$. The boundary term has been omitted, as we actually impose $\mathbf{A}_\theta = 0$ on the boundaries of Ω . From this equation, we can cast (9) as a *CFPDES* (see Fig. 1): for instance, we have $c = 1/\mu * r$.

CFPDES also includes materials definitions – e.g. physical properties and attached markers from mesh —, initial and boundary conditions, as well as multiple post-processing options to visualize or export data. The supported boundary conditions are Dirichlet, Neumann and Robin boundary conditions. All these definitions are given as JSON dictionaries structure (see Fig. 2).

C. J_c fits implementation

The critical current density of HTS material is dependent on the magnitude and orientation of \mathbf{B} and of the temperature T . The fit function describing $J_c(\mathbf{B}, \theta, T)$ and its parameters are defined in the JSON dictionary structure attached to the HTS material properties. They can also be stored in an external JSON file. This gives the possibility to replace a fit by another one, or to add more fits in the future, without modifying much the original model.

The parameters and formula of $J_c(\mathbf{B}, \theta, T)$ are written in the formalism of *Feel++*. In 2D axisymmetric coordinates, $\mathbf{B} = (-\partial_z \mathbf{A}_\theta, \partial_r \mathbf{A}_\theta + \mathbf{A}_\theta/r)$. In *Feel++*, $\mathbf{B} = (B_r, B_z)$ will be written as:

”Br” : ”-mag_grad_A_1:mag_grad_A_1”

”Bz” : ”mag_grad_A_0+mag_A/x:mag_grad_A_0:mag_A:x”

with mag_A , mag_grad_A_0 and mag_grad_A_1 respectively \mathbf{A}_θ , $\partial_r \mathbf{A}_\theta$ and $\partial_z \mathbf{A}_\theta$.

For example, the Kim's law [16]

$$J_c(\mathbf{B}) = J_{c0} / \left(1 + \sqrt{k^2 B_{\parallel}^2 + B_{\perp}^2} / B_0 \right)^\alpha \quad (11)$$

is implemented in a JSON file in Fig. 3.

TABLE I
NOUGAT

Parameters	Value
Double Pancakes	9
Turns per Pancake	290
HTS Tape width	6 mm
HTS Tape thickness	75 μm
MI thickness	30 μm
Winding inner diameter	50 mm
Winding outer diameter	109.4 mm

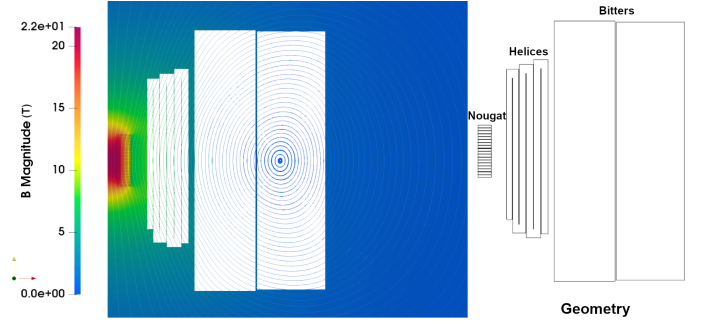


Fig. 4. Results and geometry of the T-A homogeneous model on the plateau when the transport current reaches its peak at 300 A in the HTS insert. This figure shows \mathbf{B} magnitude and streamlines for the full configuration (HTS insert, Helices & Bitter Coils). The 6 Helices and 2 Bitter Coils are made transparent for better visibility.

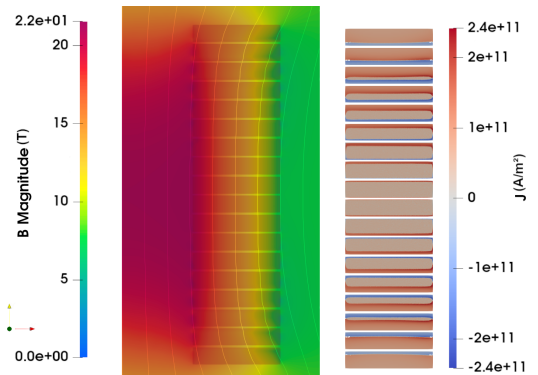


Fig. 5. Results of the T-A homogeneous model on the plateau when the transport current reaches its peak at 300 A in the HTS insert. This figure shows a close-up of the HTS insert: on the left \mathbf{B} magnitude and streamlines, on the right \mathbf{J} (A/m^2) in the insert.

IV. RESULTS

The models were validated on simple geometries (see [5]). We applied them to the Nougat insert, an HTS solenoidal coil composed of 9 stacked double pancakes [1]. More information can be found on Table I.

A. Homogeneous transient simulation

To model the Nougat insert, we need to consider 9 double-pancakes of 290 turns each. In an axisymmetric geometry, it accounts to 5 220 tapes that should be modeled individually. For such a large scale system, we use the Homogeneous method of the *T-A* formulation for HTS part. We model eighteen pancakes, on top of each other. For the resistive external field, we consider the 170 mm configuration of

high magnetic field resistive magnets available at LNCMI-Grenoble. It is a combination of 6 Helices and 2 Bitter coils that are also modeled in axisymmetric coordinates (see Fig.4).

The tapes of the HTS Nougat insert are SuperPower[®] SCS6050_AP_20 bought in 2018 and are 6mm high. To account for this superconducting material, we use the practical fit function of the critical current density versus magnetic flux density magnitude and orientation from [19] developed for SuperPower[®] superconducting tapes. The fit function is defined for a temperature of 4.2 K.

A current of 12 000 A is imposed both in the helices and in the Bitters in order to reproduce the test at 4.2 K with an 8T resistive field described in [1]. The simulation is separated in 3 parts of 30 minutes: first a ramping up to 300 A, followed by a plateau at 300 A, then a ramping down to reach 0 A.

The results for \mathbf{B} in the full configuration including the resistive magnets are presented in Fig. 4, while a close up of the HTS insert in presented in Fig. 5, representing \mathbf{B} and \mathbf{J} across the tapes. The central magnetic field reaches 21 T with 13 T generated by Nougat versus 12.9 T in [1].

B. Critical current calculation

The Nougat HTS insert is operated in a resistive background magnetic field \mathbf{B}_{bg} . To estimate the dependence of its critical current I_c versus \mathbf{B}_{bg} generated by resistive magnets, a self-consistent algorithm was implemented following [9]. To model the HTS, this algorithm uses a stationary A formulation combined with the inverted E-J power law (6).

The self-consistent algorithm is an iterative procedure computing \mathbf{J} in the tapes for different imposed current until I_c is reached. Several stopping criterions are described in [9]. The most conservative - the MAX criteria - is used here to determine I_c : I_c is defined as the current at which \mathbf{E} reaches its critical value E_c in at least one tape of the HTS insert.

The model is applied to the Nougat insert in the 170 mm configuration of helices and Bitter coils. It was computed for different values of \mathbf{B}_{bg} , with a $J_c(\mathbf{B}, \theta, T)$ fit function derived from [17] for SuperPower[®] superconducting tapes. A python iterative algorithm using a *Feel++* CFPDES toolbox was implemented.

The 5220 tapes of the insert have individual current density, used to check whether the criterion are met. Simulations are run in parallel on a personal computing environment with a 32 cores CPU and using a memory of 39 Go for 392 042 Dofs. With the MAX criterion and for 9 values of external field, the computation time is about 4 hours, which means less than half an hour for one external field.

The results are shown in the Fig. 6. I_c calculated at 4.2 K with our algorithm corresponds to the green plain line, while I_c estimation at 4.2 K from [1] are shown with the purple plain line. A 0.95% relative error is observed between the two estimates at 4.2 K confirming our results.

V. CONCLUSION

In this work, we show our beginning simulation activity of HTS magnet at LNCMI. We considered two different models: a T-A homogeneous model for transient simulation and a

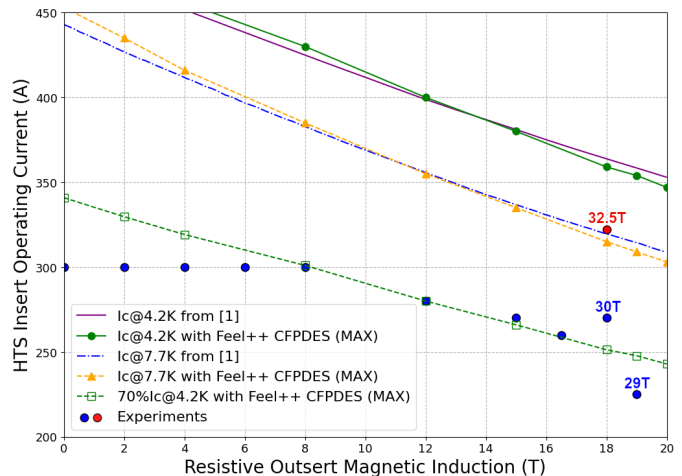


Fig. 6. HTS Nougat insert current vs. external resistive outsert magnetic induction \mathbf{B}_{bg} . The dots represent the experiments described in [1] while the lines show the computed I_c s. The green plain line and the yellow dashed line represent respectively the critical current of the HTS insert Nougat at 4.2 K and 7.7 K obtained with *Feel++* CFPDES. They use the MAX criteria from [9]. Experiments were carried out as follows: in a 1st step, the current in the HTS was set to 300 A and \mathbf{B}_{bg} was increased steadily from 0 to 8 teslas; then \mathbf{B}_{bg} was increased while the current in the HTS was decreased following a safety margin calculated on the basis of the I_c estimates at 4.2 K; finally, when \mathbf{B}_{bg} reaches 18 teslas, the current in HTS has been increased until the HTS magnet quench (red dot). At 32.5T, a slight increase in temperature in the HTS was measured and provoked the quench, indicating that the current in the insert was close to its critical limit, as shown by the 7.7 K critical lines calculated with our model and from [1].

self-consistent model to calculate the critical current. Both models were applied on the Nougat HTS insert, a magnet developed and tested in the LNCMI using a resistive magnet configuration for the background field.

We used the *Feel++* library to model the Nougat HTS in a realistic resistive outsert configuration. We obtain similar results as in experiments and with previous calculations (with a constant background field). We achieve to estimate I_c for various external background field in reasonable computational time - around 30 minutes per configuration on a 32 nodes computer -, considering the size of the system and the addition of two resistive magnets for the background field.

This library and its toolboxes allowed us to easily create algorithm using the FE models. The use of JSON dictionary structure make them flexible and straightforward to adapt for complex power-law formula. *Feel++* automatically adapts the model and the mesh to parallel computation and allows defining the solution strategy and configure the linear/non-linear algebraic solvers and preconditionner. Plus, developments that were made in this library can be integrated into LNCMI platform for running simulations with any existing resistive magnets background field. Finally, there are reduced model type toolboxes which could allow studies of sensitivity and influential parameters for I_c versus the uncertainties on the physical parameters of the J_c correlation.

Future developments with *Feel++*, will focus on adding more physics in the models: namely, consider the dependence of J_c with temperature and strain level. We also plan to simulate quenches.

REFERENCES

- [1] P. Fazilleau, X. Chaud, F. Debray, T. Lécresse, and J. Song, "38 mm diameter cold bore metal-as-insulation hts insert reached 32.5 t in a background magnetic field generated by resistive magnet," *Cryogenics*, vol. 106, p. 103053, 2020. [Online]. Available: <https://www.sciencedirect.com/science/article/pii/S0011227519304291>
- [2] F. Debray, J. Dumas, C. Trophime, and N. Vidal, "Dc high field magnets at the Incmi," *IEEE Transactions on Applied Superconductivity*, vol. 22, no. 3, pp. 4301804–4301804, June 2012.
- [3] C. Prud'homme, V. Chabannes, and al., "Feel++: Finite element embedded language and library in c++," Available at <https://www.github.com/feelpp/>.
- [4] "High temperature superconductors (hts) modelling workgroup," Available at <https://www.htsmodelling.com/>.
- [5] J. Muzet, C. Trophime, C. Prud'homme, and V. Chabannes, "Feel++ hts: <https://feelpp.github.io/feelpp-hts/feelpp-hts/latest/index.html>."
- [6] J. Dular, C. Geuzaine, and B. Vanderheyden, "Finite-element formulations for systems with high-temperature superconductors," *IEEE Transactions on Applied Superconductivity*, vol. 30, no. 3, pp. 1–13, 2020.
- [7] Z. Hong, A. M. Campbell, and T. A. Coombs, "Numerical solution of critical state in superconductivity by finite element software," *Superconductor Science and Technology*, vol. 19, no. 12, p. 1246, oct 2006. [Online]. Available: <https://dx.doi.org/10.1088/0953-2048/19/12/004>
- [8] R. Brambilla, F. Grilli, and L. Martini, "Development of an edge-element model for ac loss computation of high-temperature superconductors," *Superconductor Science and Technology*, vol. 20, no. 1, p. 16, nov 2006. [Online]. Available: <https://dx.doi.org/10.1088/0953-2048/20/1/004>
- [9] V. Zermeño, F. Sirois, M. Takayasu, M. Vojenciak, A. Kario, and F. Grilli, "A self-consistent model for estimating the critical current of superconducting devices," *Superconductor Science and Technology*, vol. 28, no. 8, p. 085004, jun 2015. [Online]. Available: <https://dx.doi.org/10.1088/0953-2048/28/8/085004>
- [10] F. Liang, S. Venuturumilli, H. Zhang, M. Zhang, J. Kvitkovic, S. Pamidi, Y. Wang, and W. Yuan, "A finite element model for simulating second generation high temperature superconducting coils/stacks with large number of turns," *Journal of Applied Physics*, vol. 122, p. 043903, 07 2017.
- [11] E. Berrospe-Juarez, V. M. R. Zermeño, F. Trillaud, and F. Grilli, "Real-time simulation of large-scale hts systems: multi-scale and homogeneous models using the t–a formulation," *Superconductor Science and Technology*, vol. 32, no. 6, p. 065003, apr 2019. [Online]. Available: <https://dx.doi.org/10.1088/1361-6668/ab0d66>
- [12] F. Grilli, "Numerical modeling of hts applications," *IEEE Transactions on Applied Superconductivity*, vol. 26, no. 3, pp. 1–8, April 2016.
- [13] A. Arsenault, B. d. S. Alves, and F. Sirois, "Comsol implementation of the h- ϕ -formulation with thin cuts for modeling superconductors with transport currents," *IEEE Transactions on Applied Superconductivity*, vol. 31, no. 6, pp. 1–9, 2021.
- [14] H. Zhang, M. Zhang, and W. Yuan, "An efficient 3d finite element method model based on the t–a formulation for superconducting coated conductors," *Superconductor Science and Technology*, vol. 30, no. 2, p. 024005, dec 2016. [Online]. Available: <https://dx.doi.org/10.1088/1361-6668/30/2/024005>
- [15] J. Rhyner, "Magnetic properties and ac-losses of superconductors with power law current–voltage characteristics," *Physica C: Superconductivity*, vol. 212, no. 3, pp. 292–300, 1993. [Online]. Available: <https://www.sciencedirect.com/science/article/pii/092145349390592E>
- [16] Y. B. Kim, C. F. Hempstead, and A. R. Strnad, "Critical persistent currents in hard superconductors," *Phys. Rev. Lett.*, vol. 9, pp. 306–309, Oct 1962. [Online]. Available: <https://link.aps.org/doi/10.1103/PhysRevLett.9.306>
- [17] J. Fleiter and A. Ballarino, "Parametrization of the critical surface of rebco conductors from fujikura," Technical report, CERN, 9 2014. Note 2014-24, EDMS no. 1426239, 2014.
- [18] M. Danial and J. Van Nugteren, "Parameterization of the critical surface of REBCO conductors from Bruker. REBCO: 2nd Generation high temperature superconductor," 2017. [Online]. Available: <https://cds.cern.ch/record/2277484>
- [19] D. K. Hilton, A. V. Gavrilin, and U. P. Trociewitz, "Practical fit functions for transport critical current versus field magnitude and angle data from (re)bco coated conductors at fixed low temperatures and in high magnetic fields," *Superconductor Science and Technology*, vol. 28, no. 7, p. 074002, jun 2015. [Online]. Available: <https://dx.doi.org/10.1088/0953-2048/28/7/074002>
- [20] C. Prud'homme, V. Chabannes, V. Doyeux, M. Ismail, A. Samake, and G. Pena, "Feel++ : A computational framework for galerkin methods and advanced numerical methods," *ESAIM: Proc.*, vol. 38, pp. 429–455, 2012. [Online]. Available: <https://doi.org/10.1051/proc/201238024>